Flux balance modelling to predict bacterial survival during pulsed activity events

Nicholas A. Jose[1], Rebecca Lau[1], Tami L. Swenson[1], Niels Klitgord[1], Ferran Garcia-Pichel[2], Benjamin P. Bowen[1], Richard Baran[1], Trent R. Northen[1]

[1]Environmental Genomics and Systems Biology Division, Lawrence Berkeley National Laboratory, Berkeley, California 5 94720, United States

[2]School of Life Sciences, Arizona State University, Tempe, Arizona 85287, United States

Correspondence to: Trent Northen (TRNorthen@lbl.gov)

Reviewer Comments

31 Oct 2017

Reviewer: The authors present a thoroughly documented manual reconstruction of Microcoleus vaginatus, a terrestrial cyanobacterium adapted to arid environments. The reconstruction is experimentally validated by comparing predicted CO2 and storage polymer production & consumption in the light and dark to measured values. The metabolic model is then exploited to predict glycogen concentration in M. vaginatus under different climate scenarios. This is solid work and I have only a few comments.
What is the number and percentage of genes with unknown functions in M. vaginatus?

Authors: Out of 5265 putative genes, there are 1990 genes (37.8%) with unknown functions from initial automated annotation. The 858 genes currently in the model are picked from initial assignments via additional annotation via the ModelSEED pipeline and manual efforts.

Reviewer: How well do the predicted fluxes during light and dark agree with previous results on gene expression in M. vaginatus-dominated BSCs?

Authors: The predicted fluxes compare well to the ones we measured in Rajeev *et al* (2013). In the light BSCs had a maximum uptake of approximately 12 – 20 µmol CO_2 g^{-1} hr^{-1}, compared to the predicted average of 11.9 µmol CO_2 g^{-1} hr^{-1}. In the dark BSCs had a maximum production of approximately 12 – 20 µmol CO_2 g^{-1} hr^{-1}, compared to the predicted average of 33.4 µmol CO_2 g^{-1} hr^{-1}. Although there is only a slight difference, the comparison is difficult to draw conclusions from because gene expression studies used BSC samples in field-like conditions, whereas our studies used *M. vaginatus* grown in isolation, constantly wetted in minimal media. In addition, because biomass was not used to normalize flux measurements in gene expression studies, an unknown biomass density needs to be assumed.

Reviewer: A delicate point in FBA is the definition of the objective function. The Materials & Methods part does not state clearly which function(s) is (are) optimised - is it biomass formation or flux through polymer-forming reactions or both? In case of biomass, how was the biomass formation reaction obtained? How well does the predicted light and dark growth rates (corresponding to the flux through the biomass formation reaction) agree with measured growth rates?

Authors: The biomass objective function is optimized. The function was initially obtained through ModelSEED, and was modified to include biopolymers in the light as a biomass requirement. The rate of total biomass accumulation was not measured, so that comparison could not be made. We do observe that the predicted growth rates scale with increasing light intensity and that in the

absence of any light in the model the predicted growth rate is 0. Both of these observations are constant with the known growth patterns of M. vaginatus.

Reviewer: Is it known whether the ratio of day/night wetting events or day length influences the distribution of M. vaginatus in deserts and arid environments?

Authors: There are no experimental studies to our knowledge that have specifically investigated the ratio of day/night wetting events. The reason for such a simulation is more to demonstrate how this model could be used given the information we have determined–carbon fluxes at fixed time intervals in the light and dark. This was inspired by the previous studies of Belnap *et al* (2003) and Reed *et al* (2012), who showed that wetting frequency and season affect the carbon balance and production of pigments for radiation-protection. A follow-up study could explore this day/night ration and wetting frequency across seasons.

Reviewer: The authors should clarify whether or not upper and lower flux bounds are constrained by measurements when predicting flux through biopolymer reactions in the dark (Table 3). How well is CO2 production and biopolymer consumption predicted without constraining flux boundaries with measurements?

Authors: Upper and lower flux bounds were constrained by the average flux measurement in the dark. The description of Table 3 has been modified to include this clarification.
Using an unconstrained flux boundary for resources (represented as positive and negative infinity for the upper and lower bound) would result in an unconstrained/infinite CO_2 flux. The purpose of constraining the FBA problem is to reduce the degrees of freedom to solve for a desired unknown flux.
Revision:
For the final version of the description for Table 3, see Reviewer #2 manuscript revisions.

Reviewer: It is curious that M. vaginatus grows so slowly (weeks) and appears to miss vital reactions. Is it possible that it relies on near-obligate mutualistic partners in nature?

Authors: *M. vaginatus* certainly has mutualistic partners in nature (and in culture) that likely facilitate more rapid growth, but they are not essential for survival because M. vaginatus may be grown axenic. The naturally slow growth is also thought to be an evolved mechanism that allows survival in harsh arid environments. The "missing" of vital reactions is more a result of annotation, where key genes in M. vaginatus lack known homologs for functional assignment.

Reviewer: Please also share the metabolic model as an SBML file. Not everyone has access to Matlab.

Authors: An SBML file has been added to the supplementary information.

Reviewer: l. 67: a terrestrial cyanobacteria -> a terrestrial cyanobacterium l. 249: which a possible reason -> which is a possible reason l. 264: there is either a 12-hour wetting event -> or?

Authors: 67 and 249 have been corrected
264: where for each day there is either a light or dark 12-hour wetting event.
Revisions (modified or added text is underlined):
L67: "a terrestrial cyanobacterium"
L249: "which is a possible reason"
L264: "there is either a light or dark 12-hour wetting event"

22 Nov 2017

Reviewer: The SBML file generates a couple of warnings when loaded with R package sybilSBML. More specifically, two reactions appear to miss an identifier (no_id) and another reaction with identifier rxn00062 occurs twice. In addition, the number of genes and metabolites displayed in R and Matlab (with iNJ1153.mat) is not the same. I hope the authors can look into these issues before publication.

Authors: Thank you for your response and apologies for the issues regarding the SBML file. Please find attached a version that should run without errors in R. Modifications were minor. The number of unique genes does not reflect the number of total genes in the model due to redundancy in annotation, where more than one gene may be associated with the same function.

5 Dec 2017

Reviewer: The authors have addressed all my concerns.

Authors: Thank you for your detailed questions and suggestions. We have amended the manuscript with the changes mentioned in previous author comments.
Revision: SBML file added to final manuscript supplementary information.

Reviewer #2

30 Jan 2018

Reviewer: Flux balance modeling to predict bacterial survival during pulsed activity events by Jose et al. This is a very interesting study where genome information is combined with detailed measurements of storage products to reach the quantitative conclusion about the cost of activity in the dark and the light. Love the paper, well written, full of new information (for me). Not being familiar with the details of genome and flux balance approaches, my questions are mostly related to clarification.

Authors: Thank you for your detailed review, insightful comments and helpful suggestions. We have included below our responses and suggested clarifications to the manuscript.

Reviewer: In the metabolic model, I assume all growth functions, such as RNA, and protein production are included? Does the model assume that these other functions, such as protein production etc, happen at similar rates during the day as during the night?

Authors: Yes, production of RNA and protein are also included. The rate of production is related to the intensity of light, so that these rates are different during the day and night.

Reviewer: The organisms were cultured at 4.5-10 umol m-2 s-1 (L83). How does this compare to the desert light levels, and how would an increase in light level affect the conclusion of this paper regarding wet/dry cycles during day/night? Is the light level PAR or total radiation?

Authors: While the radiation incident on the crust surface can be orders of magnitude higher that the one we used, it is subject to intense multiple scattering losses, so that only 1 percent of incident radiation remains a couple of millimeters down into the soil. *M. vaginatus* makes a living within this steep light gradient, usually in the subsurface, coming up to the surface only when light intensity is very moderate, (morning, overcast conditions) and it has a “shade plant” phenotype (low

photosynthesis saturation intensity, heavy complement of light harvesting pigments and no sunscreen pigments). Isolate *M. vaginatus* does not grow in liquid media under desert light levels that we used previously to mimic more natural conditions in the lab with intact biocrusts (~600 umol m-2 s-1; DOI: 10.1038/ismej.2013.83). We conducted our experiments close to the growth optimum of *M. vaginatus* in liquid media. The light level given is PAR. This text has been added to the manuscript in the methods section (section 2.2)

Revision
L85: While the radiation incident on the crust surface can be orders of magnitude higher than the one we used, it is subject to intense multiple scattering losses, so that only 1 percent of incident radiation remains a couple of millimeters down into the soil. M. vaginatus makes a living within this steep light gradient, usually in the sub-surface, coming up to the surface only when light intensity is very moderate (in morning, overcast conditions). It has a "shade plant" phenotype possessing low photosynthesis saturation intensity, heavy complement of light harvesting pigments and no sunscreen pigments. Isolate M. vaginatus does not grow in liquid media under desert light levels that we used previously to mimic more natural conditions in the lab with intact biocrusts (~600 µmol m-2 s-1) (Rajeev et al., 2013). The growth conditions used are close to the growth optimum of M. vaginatus in liquid media.

Reviewer: Related topic, in the results and discussion (L 198, 199; Table 3) two light levels are defined. It was not clear when reading the paper what this meant, whether this was caused by a change in biomass production or changed light levels. Please clarify.

Authors: Thanks for pointing this out. The manuscript has been changed to clarify this.

Revision
L83: Because different culture containers were used between respiration experiments and biopolymer experiments, they possessed different photon fluxes (measured in µmol g^{-1} h^{-1}), which is reflected in Table 3. This is accounted for in simulations.

Reviewer: L 116: please clarify why crotonic acid was determined. As far as I know, it is not mentioned in the results and discussion but seems to be the breakdown product of polyhydroxybutyrate. (?)

Authors: The manuscript has been changed to clarify this.

Revisions
Section 2.6 Title: "Quantification of PHB via LC/MS Measurement of Crotonic Acid"
L117: "Polyhydroxybutyrate breaks down to form crotonic acid in strongly acidic environments. The quantity of crotonic acid formed is used to calculate PHB quantity."

Reviewer: As a clarification, please explain why biopolymer reactions are included in the model, but not found in the genome. Similar for the other processes.

Authors: These clarifications have been added to the manuscript.

Revisions
L133: "Automatic annotations were further refined through manual annotation. This was necessary because automated modelling databases occasionally do not contain strong homologs for a certain function, and thus fail to assign it to the genome via simple homology search algorithms."

L144: "...reactions for the synthesis and metabolism of biopolymers polyphosphate, glycogen and PHB, which were not given within the automated annotation, were added after being found in the genome through extensive manual annotation."

L165: "Automated model generation typically does not assume that biopolymers act as resources that may accumulate or deplete."

Reviewer: L 150: how were LB and UB determined. On the one hand they seem to be the product of the model (Table 3) but at the same time constrain the model (L 150).

Authors: In Table 3 measured UB and LB refer to the experimental bounds, i.e. the standard deviation.
Modelled UB and LB refer to the upper and lower values obtained from sensitivity analysis. In modelled constraint reactions for light, UB and LB represent the assumed deviation that is input into sensitivity analysis.

The reaction flux UB and LB used as inputs in the model are fixed at the experimentally measured values (see L176, eqn 6). In sensitivity analysis, this is varied over the estimated deviation (See L182-186).

Due to this confusion, the LB and UB in Table 3 has been amended as seen below.

Revision
"Table 3: Experimental and modelled flux values over light and dark conditions. Constraint fluxes are noted with a "*". Negative and positive CO_2 fluxes represent uptake and respiration respectively, while negative and positive biopolymer flux rates represent depletion and accumulation respectively. Measured "-" and "+" refer to the standard deviation. Modeled "-" and "+" refer to the upper and lower values obtained from sensitivity analysis. In modeled constraint reactions for light, "-" and "+" represent the assumed deviation that is input into sensitivity analysis."

	Measured			Modeled		
	Flux ($\mu mol\ g^{-1}\ h^{-1}$)	-	+	Flux ($\mu mol\ g^{-1}\ h^{-1}$)	-	+
Light (1)						
Light*	141			141	93	211
CO_2	-19.6	-23.3	-15.9	-33.4	-50.3	-21.8
Light (2)						
Light*	4670			4670	3551	6290
Glycogen	9.99	9.47	10.51	3.07	0.00	9.30
PHB	0.0366	0.0050	0.0683	0.121	0.044	0.250
Polyphosphate	2.28	1.57	2.99	2.82	1.00	5.70
Dark						
Light*	0.00			0.00		
Glycogen*	-2.49	-6.08	1.09	-2.49	-9.66	4.67
PHB*	-0.14	-0.17	-0.11	-0.136	-0.20	-0.07
Polyphosphate*	-0.02	-1.27	1.22	-0.02	-2.51	2.46
CO_2	17.3	14.1	20.6	11.9	0	48.5

Reviewer: Table 1: what is the relevance of the reactions mentioned such as hydrogen production

in the table, but neither curated not found in the genome.

Authors: Fermentation and nitrogen fixation are known to be important pathways in biocrust metabolism. We annotated these to investigate if *M. vaginatus* could play a key role. Hydrogen production was annotated because hydrogen evolution was measured from crusts in previous experiments, though not reported.

Reviewer: L 170-173 and Table 2: I am not familiar with flux balance calculations, so the phrase PHB -> nothing is confusing? Please add explanation in one additional sentence.

Authors: This has been changed.

Revision:
L167: "…where A is a side reactant,B is a side product, X is a polymer subunit, and X_n is a polymer with length n. 'Nothing" is not a physical term, but a mathematical way to describe resource accumulation in a steady state simulation."

Reviewer: Table 3 and Fig. 2c seem to have some overlap.

Authors: This is true, they are just different representations of the same data, we've decided it best to keep them because they may be useful to different types of readers. While the graph provides a visual comparison of experiment and model predictions, the tabulation of values may be helpful for those performing future simulations and studies.

Reviewer: L 214: please elaborate how polyP can be used in other ways than an energy source

Authors: This has been corrected as described below:
Revision
L213-214: "Polyphosphate is likely an important biopolymer for *M. vaginatus* across many different stressed conditions as a reservoir of phosphate for later growth, though so-called "luxury uptake" and storage when growth is halted by some other factor, and as a reservoir of energy in the form of phosphate-phosphate bonds under conditions of abundant energy generation, phosphate and a lack of conditions to use it for growth or homeostasis. This importance of polyphosphate has been identified in gene expression studies (Rajeev et al., 2013)."

Reviewer: L 218: change consistent to constant or words similar to that.

Authors: Done

Revision
L218: "…storage polymer or for other metabolic activities that do not require a constant energy source, such as replication."

Reviewer: L 52: diel does not need to be capitalized

Authors: Done

Revision
L52: "During the diel cycle…"

Reviewer: L 63: the use of the phrases dark and light reactions are confusing: they have very

specific meaning in the study of photosynthesis, but I don't think that is what is meant here. Please Â˘n replace with something like metabolism in the dark versus in the light.

Author: Good point. We avoid those terms now in the manuscript to avoid confusion.

Revision
L63: "Therefore, we expect wet-up and dry-down metabolism in the dark likely have fixed biopolymer costs whereas metabolism in the light enables replenishment of biopolymer reserves."

Reviewer: L71: complex sentence that can be simplified.

Author: Done

Revision:
L70-71: "We interpret these results using a simple cost/benefits framework. The "cost" is biopolymer depletion in the dark, and the "benefit" is biopolymer accumulation in the light.

Reviewer: L 94: add rcf to the list of abbreviations, and add units

Author: Done. Changed to "x g" (g-force). All units will be added to the abbreviations.

Revisions:
Abbreviations (L284):

GPR	Gene-Protein-Reaction
PAR	Photosynthetically Active Radiation
Units	
Å	Angstrom
g	gram
h	hour
L	liter
m	meter
M	moles per liter
mg	milligram
min	minute
mL	milliliter
mm	millimetre
mmol	millimole
mol	mole
rpm	rotations per minute
s	second
x g	g-force (x 9.81 m s^{-2})
µg	microgram
µL	microliter
µm	micrometer
µmol	micromole

Reviewer: L 134: what are GPR relations

Author: The Gene-Protein-Reaction relation. It is a standardized description of the link between a gene, its associated protein, and the associated reaction in genome-scale metabolic models. We include this in abbreviations.

Revision
Abbreviations (L284):
GPR Gene-Protein-Reaction
PAR Photosynthetically Active Radiation

Reviewer: L 135: comma after databases can be removed

Author: Done
Revision
L135: "…analysis, and the databases KEGG and MetaCyc…"

Reviewer: L 168: why the word "side" with reactant and product?

Author: The reactants and products of interest are the biopolymer and its subunit. A and B are used to generalize other chemicals involved in the process.

Reviewer: L 194: change profiles to concentrations

Author: Done
Revision
L194: "…carbon dioxide profiles concentrations varied linearly with time…"

Reviewer: L 246: Add year after reference (Knoop)

Author: Done
Revision
L246: "(Knoop *et al.*, 2013)"

Reviewer: L 247: is the efficiency measured at the same light level?

Author: No, the rates are normalized to the photon intensity in this comparison.

Flux balance modelling to predict bacterial survival during pulsed activity events

Nicholas A. Jose[1], Rebecca Lau[1], Tami L. Swenson[1], Niels Klitgord[1], Ferran Garcia-Pichel[2], Benjamin P. Bowen[1], Richard Baran[1], Trent R. Northen[1]

[1]Environmental Genomics and Systems Biology Division, Lawrence Berkeley National Laboratory, Berkeley, California 94720, United States

[2]School of Life Sciences, Arizona State University, Tempe, Arizona 85287, United States

Correspondence to: Trent Northen (TRNorthen@lbl.gov)

Abstract

Desert biological soil crusts (BSCs) are cyanobacteria-dominated, surface soil microbial communities common to plant interspaces in arid environments. The capability to significantly dampen their metabolism allows them to exist for extended periods in a desiccated dormant state that is highly robust to environmental stresses. However, within minutes of wetting, metabolic functions reboot, maximizing activity during infrequent permissive periods. *Microcoleus vaginatus*, a primary producer within the crust ecosystem and an early colonizer, initiates crust formation by binding particles in the upper layer of soil via exopolysaccharides, making microbial dominated biological soil crusts highly dependent on the viability of this organism. Previous studies have suggested that biopolymers play a central role in the survival of this organism by powering resuscitation, rapidly forming compatible solutes and fuelling metabolic activity in dark, hydrated conditions. To elucidate the mechanism of this phenomenon and provide a basis for future modelling of BSCs, we developed a manually-curated, genome-scale metabolic model of *Microcoleus vaginatus* (iNJ1153). To validate this model, GC/MS and LC/MS were used to characterize the rate of biopolymer accumulation and depletion in in hydrated *Microcoleus vaginatus* under light and dark conditions. Constraint-based flux balance analysis showed agreement between model predictions and experimental reaction fluxes. A significant amount of consumed carbon and light energy is invested into storage molecules glycogen and polyphosphate, while β-polyhydroxybutyrate may function as a secondary resource. Pseudo-steady state modelling suggests that glycogen, the primary carbon source with the fastest depletion rate, will be exhausted if *M. vaginatus* experiences dark wetting events four times longer than light wetting events.

1 Introduction

BSCs, estimated to contain ~4.9 Pg of terrestrial carbon globally, play critical roles in stabilizing the soil in desert and arid lands that comprise nearly 40% of planetary dry land masses (Garcia-Pichel et al., 2002;Elbert et al., 2012). BSCs exist in a desiccated and metabolically dormant state that is highly robust to environmental stresses, yet are able to rapidly re-boot metabolism within minutes of wetting enabling them to capitalize on infrequent pulsed activity events that occur upon wetting (Garcia-Pichel et al., 2013). The scale and potential sensitivity of BSCs to temperature and wetting frequency/duration make them particularly relevant to understanding the impact of climate change on soil microbial communities (Grote et al., 2010). Climate models predict alterations in precipitation frequency, intensity and seasonality all of which may negatively impact BSCs given that they often exist on the fringe of habitability (Belnap et al., 2004;Johnson et al., 2012). The validity of this concern has been experimentally validated by Reed et al., who showed a demise of mosses from BSCs when exposed to frequent low-intensity wetting events (Reed et al., 2012).

Pioneering cyanobacteria, such as *Microcoleus vaginatus*, initiate the formation of BSCs by binding particles in the upper layers of the soil with polysaccharide fibers (Garcia-Pichel and Wojciechowski, 2009). This not only stabilizes the soil, but creates a local environment that is conducive to diverse succession of microbes. However, development of mature

crusts from raw soils is a slow process, typically taking many years and presenting many challenges to environmental restoration efforts. The reason for this phenomenon is not well understood, but has been ascribed to the limited and sporadic periods of growth. Presumably BSC organisms have evolved to capitalize on wetting events that range from several hours to a few days, and appear to be poised to immediately restart metabolism (Potts, 1999). Indeed, after re-hydration, BSC microorganisms start respiration within seconds, photosynthesis within minutes, and nitrogen fixation within tens of minutes (Rajeev et al., 2013;Garcia-Pichel and Belnap, 1996). Somewhat paradoxically, isolates of *M. vaginatus* grown in idealized laboratory conditions are still extremely slow-growing with doubling times of weeks. This may be a result of ingrained evolutionary pressures that prioritize robustness to various environmental stresses over growth.

Previous studies on the desiccation cycle in *M. vaginatus* based on transcript analysis in intact BSCs indicated multiple metabolic states (Rajeev et al., 2013). These states are associated with genes responsible for biopolymer formation and depletion, such as cyanophycin, glycogen, β-polyhydroxybutyrate (PHB), and polyphosphate. Wetting of dry crusts results in increased expression in genes for sugar transporters and biopolymer biosynthesis. During the dD~~D~~iel cycle, the expression patterns of biopolymer-associated genes suggest that depletion occurs at night and accumulation during the day. Drying resulted in elevated expression of genes involved in biopolymer metabolism, including glycogen breakdown. Together these observations reinforce the centrality of osmolytes and biopolymers in the *M. vaginatus* desiccation cycle. Consistent with this view, our recent D_2O labelling study of wetted *M. vaginatus* and *Synechococcus sp.* 7002 revealed that in light, low-growth, constant osmotic conditions many osmolytes are rapidly turned over (Baran et al., 2017). To gain insights into this process, stable isotope probing experiments were performed using the osmolyte glucosylglycerol, showing that *Synechococcus sp.* 7002 rapidly converts this osmolyte into glycogen. This suggests a mechanism where high fluxes of compatible solutes are maintained through conversion to biopolymers. This high flux would enable cells to survive rapid desiccation by simultaneously turning off compatible solute polymerization and mobilizing biopolymer hydrolysis. Therefore, we expect wet-up and dry-down metabolism in the dark likely have fixed biopolymer costs whereas metabolism in the light enables replenishment of biopolymer reserves.~~wet-up, dry-down and dark reactions likely have fixed biopolymer costs whereas the light reactions enable replenishment of biopolymer reserves~~. Given the importance of biopolymers to *M. vaginatus*, the balance of costs vs. accumulation could be used to predict net carbon accumulation and survival of *M. vaginatus* during various climate scenarios.

Here, as a first step towards this goal, we constructed a genome-scale metabolic network of *M. vaginatus* (iNJ1153). To our knowledge, this is the first for a terrestrial cyanobacteri~~a~~um and describes a flux balance approach that accounts for biopolymer accumulation using polyphosphate, β-polyhydroxybutyrate (PHB), and glycogen, important storage molecules and osmolytes (Diamond et al., 2015). We use this model in combination with direct measurements of biopolymer concentrations and carbon dioxide flux to examine dark and light flux distributions in *M. vaginatus*. We interpret these results using a simple cost/benefits framework. The "cost" is biopolymer depletion in the dark, and the "benefit" is biopolymer accumulation in the light.~~for biopolymer depletion in the dark 'costs' and accumulation in the light 'benefits'.~~

2 Materials and Methods

2.1 Chemicals

Potassium phosphate (dibasic) (CAS 7758-11-4), crotonic acid (CAS 107-93-7), D-glucose (CAS 50-99-7), 98% methoxyamine hydrochloride (CAS 593-56-6), pyridine (CAS 110-86-1), fatty acid methyl ester (FAME) standards (kit ME10-1KT) and LC/MS-grade acetonitrile (CAS 75-05-8) were from Sigma (St. Louis, MO). LC/MS grade water was from JT Baker. N-methyl-N-(trimethylsilyl)-trifluoroacetamide (MSFTA) containing 1% trimethylchlorosilane was from Restek (Bellafonte, PA).

2.2 Culturing

M. vaginatus PCC 9802 was grown at 22 ºC in minimal Jaworski's media with a 12-hour light, 12-hour dark cycle. Light was provided by a 6500 K, 2000 lumen fluorescent source. Light flux measured at the level of the petri dishes was approximately 4.5-10 µmol photons m^{-2} s^{-1} PAR. Because different culture containers were used between respiration experiments and biopolymer experiments, they possessed different photon fluxes (measured in µmol g^{-1} h^{-1}), which is reflected in Table 3. This is accounted for in simulations. A minimum of 3 replicates grown at identical conditions were used for each experiment. To determine the biopolymer flux rates, 3 samples were taken at the start and end of 12 hours growing at a given condition.

While the radiation incident on the crust surface can be orders of magnitude higher than the one we used, it is subject to intense multiple scattering losses, so that only 1 percent of incident radiation remains a couple of millimeters down into the soil. M. vaginatus makes a living within this steep light gradient, usually in the sub-surface, coming up to the surface only when light intensity is very moderate (in morning, overcast conditions). It has a "shade plant" phenotype possessing low photosynthesis saturation intensity, heavy complement of light harvesting pigments and no sunscreen pigments. Isolate M. vaginatus does not grow in liquid media under desert light levels that we used previously to mimic more natural conditions in the lab with intact biocrusts (~600 µmol m-2 s-1) (Rajeev et al., 2013). The growth conditions used are close to the growth optimum of M. vaginatus in liquid media.

2.3 Respiration Measurement

Carbon dioxide flux was determined from three biological replicates in both light and dark conditions with a Micro-Oxymax Respirometer (Columbus Instruments) in sealed 100 mL mason jars. The system monitored carbon dioxide accumulation across all samples over a 48-hour period with a time resolution of approximately 48 minutes per measurement. These values are scaled to µmol/gram biomass.

2.4 Biopolymer Extraction

Immediately following respiration measurements, triplicate aliquots of *M. vaginatus* cultures (1 mL) from both light and dark conditions were removed and transferred to a pre-weighed 1.5 mL tube. Cells were pelleted by centrifuging at 3000 rcf for 3 min, resuspended in 1 mL methanol and homogenized with sterile metal ball bearings using a Mini-Beadbeater (BioSpec Products). Samples were centrifuged at 3000 rcf for 3 min and supernatant discarded. Homogenization and centrifugation were repeated for a total of three times. The remaining biomass was dried in a Savant SpeedVac SPD111V and dry weight was measured. To allow efficient hydrolysis of polyphosphate, glycogen, and PHB, 500 µL of 2M HCl was added and the mixture heated at 95°C for 1 h while shaking (1400 rpm) (Dephilippis et al., 1992;Eixler et al., 2005;Ernst and Boger, 1985). Samples were then dried and resuspended in 1 mL methanol by vortexing and bath sonication (VWR Symphony). Samples were cleared of any remaining cells by centrifuging at 3000 rcf for 3 min and filtered through 0.22 µm centrifugal filters (Nanosep MF, Pall Corporation, Port Washington, NY).

2.5 GC/MS Measurement of Glucose and Phosphate

An aliquot of the hydrolyzed biopolymers (10% of the original biomass) was dried for GC/MS analysis of glucose and phosphate. To each dried sample, 10 µL of 40 mg/mL methoxyamine hydrochloride in pyridine was added. The mixture was shaken for 1.5 h at 30°C and 1400 rpm. FAME standards (1 µL) (Swenson et al., 2015) in 90 µL MSTFA were added to each sample and standard. The mixture was shaken at 37°C for 30 minutes and 1400 rpm. The contents were then transferred to glass vials with micro-inserts and submitted to GC-MS analysis.

GC/MS data were acquired on an Agilent 7890 gas chromatograph (Agilent Technologies, Santa Clara, CA) and an Agilent 5977 single quadrupole as described in Swenson et al, 2015. In summary, derivatized samples were injected (0.2-0.5 µL) using a Gerstel automatic liner exchange MPS system (Gerstel, Muehlheim, Germany) into a Gerstel Cooled Injection System (CIS4) operated in splitless mode. Analytes were separated using a Rxi-5Sil MS capillary column (Restek, Bellefonte, PA) with a 0.25 mm ID Integra Guard under an initial oven temperature of 60°C, held for 1 min then ramped at 10°C/min to 310°C with a total runtime of 36 min. Glucose was detected as two peaks at 17.5 and 17.7 min and phosphate at 10.0 min. Glucose and phosphate were quantified based on a 5-point standard curve (in triplicate) from 0.5-10 µg. All measurements fell within the linear range. Calculated concentrations were then normalized to original dried biomass.

2.6 Quantification of PHB via LC/MS Measurement of Crotonic Acid

Polyhydroxybutyrate breaks down to form crotonic acid in strongly acidic environments. The quantity of crotonic acid formed is used to calculate PHB quantity. Crotonic acid was measured by LC-MS/MS on an Agilent 1290 UHPLC (Agilent Technologies, Santa Clara, CA) coupled to a Q-Exactive mass spectrometer (Thermo Scientific, San Jose, CA). A sample volume of 2 µL was injected onto a Kinetix C18-XB column (150mm x 2.6µ x 100Å) (Phenomenex, Torrance, CA),

and eluted over a linear gradient of water + 0.1% formic acid (FA) (A) to acetonitrile + 0.1% FA (B), with an initial 1 min hold at 100% A, a 7-min gradient to 100% B, followed by a 1.5 min hold at 100% B, and a 2-min re-equilibration at 100% A. Crotonic acid eluted at 2.2 min, and was detected in positive mode. Crotonic acid was quantified based on a 5-point standard curve (in triplicate) using the parent ion (87.0447 m/z in positive mode), and all sample measurements fell within the linear range (10 ng/mL to 100 µg/mL). Crotonic acid concentrations were normalized to original dry biomass weights.

2.7 Metabolic Network Reconstruction and Refinement

The genome of *M. vaginatus* PCC 9802 was first sequenced by the US Department of Energy Joint Genome Institute. The draft reconstruction of this genome was obtained using the Model SEED, a pipeline for generating metabolic models from genome data (Henry et al., 2010). The genome was automatically annotated using RAST (Overbeek et al., 2014). A reaction network complete with gene-protein-reaction relationships, predicted Gibb's free energy of reaction values, and an organism specific biomass reaction including non-universal cofactors such as wall components and lipids was generated. This network was also converted into its mathematical form, allowing quantitative systems biology analysis via flux balance analysis (FBA).

Automatic annotations were further refined through manual annotation. This was necessary because automated modelling databases occasionally do not contain strong homologs for a certain function, and thus fail to assign it to the genome via simple homology search algorithms. Extensive manual refinement was performed to examine RAST predicted functions, GPR relations, and fill gaps in metabolic pathways. Detailed manual annotation reports can be seen in supplementary information. This was performed using literature review, flux balance analysis, and the databases~~,~~ KEGG and MetaCyc (Kanehisa and Goto, 2000; Karp et al., 2002). Flux balance analysis was run using the COBRA Toolbox (Becker et al., 2007). The refinement process is illustrated in Figure 1.

M. vaginatus' biochemical capabilities are relatively unstudied in literature to date, hence, strong sequence homology to related bacterial enzymes and to previous literature findings, were used as criteria in assigning functionalities, gene-protein-reaction relationships, and reaction directionalities. Although photosynthetic genes were identified via automatic annotation, photosynthetic reactions were not present in the generated mathematical model. To reconcile this, and given the fact that only a few models exist for cyanobacterial oxygenic photosynthesis, the model of photosynthesis developed for the cyanobacterium *Cyanothece* sp. ATCC 51142 (iCce806) was adopted (Vu et al., 2012). In addition, to enable the analysis of biopolymer fluxes, reactions for the synthesis and metabolism of biopolymers polyphosphate, glycogen and PHB ~~were added~~, which were not given within the automated annotation, were added after being found in the genome through extensive manual annotation.

Constraint based flux balance analysis is a common approach that abstracts the metabolic capabilities of an organism as a set of linear equations, then uses constraint based linear optimization to predict the pathway usage and flux through a network (Orth et al., 2010). In this study, a pseudo-steady state approximation Eq. (1) is used, where the

accumulation of each metabolite is zero over time. $\boldsymbol{S}$ is the stoichiometric matrix of equations, and $\boldsymbol{v}$ is the vector of flux values. The flux is constrained by upper and lower bound vectors, $\boldsymbol{LB}$ and $\boldsymbol{UB}$, in Eq. (2).

$$S \cdot v = 0\,, \tag{1}$$

$$LB \leq v \leq UB, \tag{2}$$

Model metabolites were separated into the extracellular and cytosol (inner) domains. Sink reactions simulated transport between the environment and extracellular domains, while exchange reactions mediated transport between extracellular and cytosol domains.

Despite initial manual curation efforts, the model was initially unable to simulate photoautotrophic growth using a minimal media using the biomass reaction from ModelSEED. A minimal media is defined as only containing essential trace minerals, oxygen, carbon dioxide, light, sulphate, and nitrate/ammonium. Missing precursors, mainly, thiamine-phosphate, L-cysteine, and spermidine, were found to prevent growth. Using the databases, KEGG and MetaCyc, possible reactions that allow *M. vaginatus* to produce biomass were identified in a process known as "gap-filling." Once found, these functions were cross-checked to determine if they were predicted with lower homology in *M. vaginatus'* genome, and common in related cyanobacteria. If these criteria were not fulfilled, but the function was absolutely required, the reaction was still incorporated in the model with a low confidence rating.

2.8 Modelling Biopolymer Accumulation and Utilization

Automated model generation typically does not assume that biopolymers act as resources that may accumulate or deplete. Modelling biopolymer depletion was accomplished by treating biopolymer subunits as bounded external resources. In other words, instead of the typical accumulation reaction, "pool" reactions, Eq. (4) and Eq. (5), were created for each biopolymer, where A is a side reactant, B is a side product, X is a polymer subunit, and X_n is a polymer with length n. "Nothing" is not a physical term, but a mathematical way to describe resource accumulation in a steady state simulation. The sink reaction, Eq. (5), then allows the model to undergo steady state simulation. The fluxes through the sink reactions from FBA simulation represent rates of accumulation or depletion.

$$X \mathrel{+}\!\!\rightarrow X_n + B, \tag{4}$$

$$X_n + X + A \leftrightarrow\!\!\mathrel{+} X_{n+1} + B, \tag{3}$$

$$X_n \rightarrow nothing, \tag{5}$$

To predict respiration in the dark, the light flux rate was set to 0 and biopolymer flux rates were constrained by the experimentally determined values. To set the flux of an individual reaction, Eq. (6) was used, where UB_i and LB_i are the upper and lower constraints of reaction i, and ${v_i}^{exp}$ is the measured flux.

$$UB_i = LB_i = {v_i}^{exp}, \tag{6}$$

Modelling biopolymer accumulation under light was accomplished by including biopolymer requirements within the biomass objective function, according to their stasis levels as measured during experiments. Biopolymer accumulation rates can then be calculated using the simulated biomass accumulation rate.

The ability of the constructed network to quantitatively predict metabolic activity was assessed by comparing the calculated rates of respiration in the dark and CO_2 uptake and biopolymer accumulation in the light, with the experimentally determined values.

To address the issue of biological variation across samples and their impact on model predictions, sensitivity analysis was performed on the flux constraints. Biopolymer constraints were varied within two standard deviations of the average measured value, light flux levels were varied within ± 1 µmol photons m^{-2} s^{-1}, and biomass levels were varied within ± 2 mg. A total of 30,619 different simulations were performed in this analysis.

3 Results & Discussion

3.1 Metabolic Network Reconstruction

The resulting reconstructed genome scale model possesses 858 genes, 1153 reactions, and 1078 metabolites. A total of 146 reactions were added from manual curation, gap analysis, and for biopolymer simulations of polyphosphate, glycogen, and PHB. For a comparison of the automated and curated annotation see Table 1. Added biopolymer reactions are shown in Table 2~~Table 2~~. To view the model in Excel and Matlab structure formats see the supplementary information.

Formatted: Font: 10 pt, Not Bold

3.2 Experimentally Determined Fluxes ~~During~~during Photosynthesis and Respiration

In both light and dark conditions, carbon dioxide ~~profiles~~ concentrations varied linearly with time, supporting the assumption that *M. vaginatus'* metabolism behaves like a quasi-steady-state system over 12-hour time cycles. It also indicates that using experimental data to validate and constrain a steady state flux balance model is reasonable in a 12-hour time scale.

With a light flux of approximately 141 µmol/mg/h, *M. vaginatus* accumulated carbon dioxide at approximately 19.6 ± 3.7 µmol/g biomass/hour. Without light, it released carbon dioxide at 17.3 ± 3.2 µmol/g biomass/hour. The biopolymer flux rates in the dark and under a light flux of 4670 µmol/mg/h are reported in Table 3.

Interestingly, the rate of glycogen depletion in the dark is approximately a quarter of the rate of accumulation in the light. For these conditions, *M. vaginatus* has a conservative metabolism, accumulating much more biopolymer in a day than is necessary for the following night. We can speculate that biopolymer reserves may be accumulated such that sufficient quantities may drive physiological responses such as cell division, making it akin to the yeast metabolic cycling observed for low glucose conditions (Yin et al., 2003). Since this photoautotroph is limited by nutrients other than carbon, they are likely

routing flux from intracellular biopolymers into EPS formation, consistent with our earlier results showing export of a diversity of oligosaccharides (Baran et al., 2013).

Gene expression studies showed increased expression of hydrolytic enzymes (e.g. glycogen debranching enzyme) during dry-down which may provide a mechanism to rapidly produce compatible solutes (Baran et al., 2017). These are presumably excreted during wet-up resulting in an additional metabolic cost for wet-up that must be recouped through biopolymer accumulation. Thus, the observed high flux to glycogen may provide multiple physiological adaptations that are critical to survival in arid climates.

Polyphosphate possesses an uptake rate like that of the glycogen, but is only depleted 1% as fast in the dark, indicating that this resource is conserved quite well. Polyphosphate is likely an important biopolymer for M. vaginatus across many different stressed conditions, as a reservoir of phosphate for later growth, though so-called "luxury uptake" and storage when growth is halted by some other factor, and as a reservoir of energy in the form of phosphate-phosphate bonds under conditions of abundant energy generation or a lack of conditions to use it for growth or homeostasis. This importance of polyphosphate has been identified in gene expression studies~~and may be used in other ways than as an energy source, which agrees with gene expression studies~~ (Rajeev et al., 2013).

PHB accumulates at roughly 0.4 % of the rate that glycogen accumulates, indicating that it is not the primary polymer used for storage. Interestingly, its depletion rate is higher than its accumulation rate. It may be used as a secondary storage polymer or for other metabolic activities that do not require a ~~consistent~~ constant energy source, such as replication. The study of PHB over multiple light/dark and dry/wet cycles may be crucial to understanding the role that PHB plays.

Although each bacterial sample was taken from the same culture, variation in metabolic activity existed regardless of dry biomass normalization. This may be attributed to differing amounts of polysaccharide sheaths surrounding active cells (Bertocchi et al., 1990). The large amounts of exopolysaccharides in *M. vaginatus (Hokputsa et al., 2003)*, which are considered distinct in chemical form and function from glycogen, may also interfere with GC-MS quantification of storage glucose. A complete study of EPS composition in *M. vaginatus* has yet to be completed in the authors' existing knowledge. Therefore, we have limited our analysis to using these measurements as the upper and lower bounds on metabolic fluxes. Improvements in methods for quantifying glucose levels from glycogen without EPS bias will be important for further model refinement as would be extension of the model to include EPS.

3.3 Simulation Results and Experimental Validation

A comparison of simulation and experimental CO_2 accumulation rates can be seen in Figure 2. In the dark, the predicted average carbon dioxide flux was 11.9 µmol/day/g, close to the measured value of 17.3 ± 3.2 µmol/day/g. In the light, the predicted average carbon dioxide uptake flux using the measured light flux as a constraint was -33.4 µmol/g biomass/hour, compared to the experimental value of -19.6 ± 3.7. Sensitivity analysis showed that the variation in biopolymer flux measurements, illumination, and biomass could account for this variation.

Accumulation rates of polyphosphate and PHB fall within the range predicted by simulation. The average simulated glycogen accumulation is lower than the experimentally measured glycogen accumulation rate, though sensitivity analysis may account for this. Another possible reason for this lower estimate could be that *M. vaginatus* biomass requirements are less than the requirements given by ModelSEED. To verify the biomass composition a more thorough investigation may be conducted.

From the modelled fluxes, we estimate that under constant wetted conditions, *M. vaginatus* routes 2% of its carbon uptake to the generation of storage glycogen and PHB, while the rest may be attributed to cell maintenance, biomass growth, or other unknown storage molecules. Although this value is expected to change depending on growth conditions, it provides a basis for future studies. Further analysis of the network fluxes may prove useful in investigating potentially important pathways in *M. vaginatus*' metabolism. For such studies, flux information from light and dark experiments across all reactions ~~have~~has been included in the supplementary section.

Compared to the modelled metabolism of *Synechocystis* sp. PCC 6803 (Knoop et al., 2013)~~modelled by Knoop *et al*~~, CO_2 uptake and glycogen accumulation per photon of light are 2.5 and 5.7 times faster respectively. Glycogen depletion in the dark is only 36% faster. The accelerated accumulation of carbon indicates that *M. vaginatus* may have a more efficient pathway for converting CO_2 to biopolymer storage, which is a possible reason for its role as a pioneer organism in BSCs.

3.4 Survivability during Pulsed Activity Events

BSCs are vulnerable to alteration in wetting events (Reed et al., 2012). This coupled with predictions of alterations in rainfall and increasing aridity in biocrust habitats (Maestre et al., 2015a;Maestre et al., 2015b) makes it important to develop tools to predict survival under changing rainfall and light intensity. Towards this goal, we can use the results from our model as a crude estimate of the 'health' of *M. vaginatus* based on biopolymer levels. Certainly, this is overly simplistic and there are many other factors that impact 'health'. However, given the central role of biopolymers in surviving in the dark and producing compatible solutes, their levels are expected to be critical to survival. Because glycogen, the primary carbon biopolymer, is consumed at about 25% of the accumulation rate, if wetting events in the dark are more than four times as long as wetting events in the light, *M. vaginatus*' health would begin to deteriorate. For lower light intensities than the ones used here, the rate of glycogen accumulation would decrease, reducing *M. vaginatus* resistance to persistent dark wetting events.

The model constructed here may be applied to more complicated, dynamic events, such as those with varied intensities of light and wetting time. To illustrate how this might be achieved, we simulated glycogen depletion over 100 days for various wetting frequencies in the light and dark, seen in Figure 3, where for each day there is either a 12-hour wetting event. When the ratio of light:dark events of 1:3, glycogen storage is maintained, whereas at 1:1 accumulation is rapid. At 1:5 glycogen stores become depleted after 94 days. This simulation may be improved in future studies by considering dynamic responses to light variation as well as the drying and re-wetting of soil.

Conclusions

We have generated the first reconstruction of the *M. vaginatus* metabolic network through careful manual annotation and inclusion of biopolymer reactions known to be important to cyanobacterial physiology. We use the model within a conceptual framework of "costs" and "benefits" associated with specific environmental changes. More precisely, we observed that dark reactions have a 'cost' which is recouped during light reactions. Using these experimental constraints on biopolymer and light fluxes, the model generates CO_2 and biopolymer fluxes that match experimental results. Using this model and laboratory experiments we found that, in light, 2% of carbon uptake is routed to storage polymers via photosynthesis. In the dark, glycogen functions as the primary carbon source. Using depletion and accumulation rates, we then predicted the gradual depletion of *M. vaginatus'* biopolymer reserves if dark wetting events were four times as long as light wetting events. This work lays the foundation for additional research on this important desert microbe and its microbial community. Since *M. vaginatus* is a keystone organism in many biocrusts, ~~it's~~its loss would have a major impact on the community. Yet, it is important to emphasize that these laboratory experiments are a vast extrapolation from native conditions and future work will focus on extending these models to more realistic environmental conditions. Additional steady-state experiments using different growth conditions found in desert environments—varying lighting intensities, levels of moisture, soil compositions, and other microbial interactions—have the potential to refine the model and identify key metabolic states related to resuscitation and dormancy to more accurately model environmental responses.

Abbreviations

BSC	Biological Soil Crust
EPS	Exopolysaccharides
FBA	Flux Balance Analysis
GC/MS	Gas Chromatography Mass Spectrometry
GPR	Gene-Protein-Reaction
Acc~~.~~	Accumulation
Resp~~.~~	Respiration
Chemicals	
ADP	Adenosine diphosphate
ATP	Adenosine triphosphate
FAME	Fatty Acid Methyl Ester
Gly	Glycogen
MeOX	Methoxyamine hydrochloride
MSFTA	N-methyl-N-(trimethylsilyl)-trifluoroacetamide
PAR	Photosynthetically Active Radiation

PHB	β-polyhydroxybutyrate
~~Gly~~	~~Glycogen~~
PP	Polyphosphate

Notation

A	generic side reactant
B	generic side product
LB_i	Flux lower bound of reaction i
$\boldsymbol{LB}$	Vector of flux lower bound values
P	phosphate level
S	Stoichiometry matrix of reaction equations
UB_i	Flux upper bound of reaction i
UB	Vector of flux upper bound values
v_i^{exp}	Experimentally determined flux value of reaction i
v	Vector of flux values
X	Polymer precursor
X_n	Polymer subunit

Units

Å	**Angstrom**
g	**gram**
h	**hour**
L	**liter**
m	**meter**
M	**moles per liter**
mg	**milligram**
min	**minute**
mL	**milliliter**
mm	**millimetre**
mmol	**millimole**
mol	**mole**
rpm	**rotations per minute**
s	**second**
x g	**g-force (x 9.81 m s-2)**
µg	**microgram**
µL	**microliter**

Formatted: Font: Italic

µm micrometer

µmol micromole

Competing interests

The authors declare that they have no conflict of interest.

Acknowledgements

We acknowledge the contribution of Seth Axen, Rahul Basu, Kriti Sondhi, and David Soendjojo with their assistance annotating the *M. vaginatus* genome. This work was supported in part by previous breakthroughs obtained through the Laboratory Directed Research and Development Program of Lawrence Berkeley National Laboratory supported by the US Department of Energy Office of Science and through the US Department of Energy Office of Science, Office of Biological and Environmental Research Early Career Program (award to T.R.N.) both under contract number and DE-AC02-05CH11231.

References

Baran, R., Ivanova, N. N., Jose, N., Garcia-Pichel, F., Kyrpides, N. C., Gugger, M., and Northen, T. R.: Functional genomics of novel secondary metabolites from diverse cyanobacteria using untargeted metabolomics, Mar Drugs, 11, 3617-3631, 10.3390/md11103617, 2013.

Baran, R., Lau, R., Bowen, B. P., Diamond, S., Jose, N., Garcia-Pichel, F., and Northen, T. R.: Extensive Turnover of Compatible Solutes in Cyanobacteria Revealed by Deuterium Oxide (D2O) Stable Isotope Probing, ACS Chem Biol, 12, 674-681, 10.1021/acschembio.6b00890, 2017.

Becker, S. A., Feist, A. M., Mo, M. L., Hannum, G., Palsson, B. O., and Herrgard, M. J.: Quantitative prediction of cellular metabolism with constraint-based models: the COBRA Toolbox, Nature Protocols, 2, 727-738, 10.1038/nprot.2007.99, 2007.

Belnap, J., Phillips, S. L., and Miller, M. E.: Response of desert biological soil crusts to alterations in precipitation frequency, Oecologia, 141, 306-316, 10.1007/s00442-003-1438-6, 2004.

Bertocchi, C., Navarini, L., Cesaro, A., and Anastasio, M.: Polysaccharides from cyanobacteria 1, Carbohydrate Polymers, 12, 127-153, 10.1016/0144-8617(90)90015-k, 1990.

Dephilippis, R., Sili, C., and Vincenzini, M.: Glycogen and poly-beta-hydroxybutyrate synthesis in spirulina-maxima, Journal of General Microbiology, 138, 1623-1628, 1992.

Diamond, S., Jun, D., Rubin, B. E., and Golden, S. S.: The circadian oscillator in Synechococcus elongatus controls metabolite partitioning during diurnal growth, Proc Natl Acad Sci U S A, 112, E1916-1925, 10.1073/pnas.1504576112, 2015.

Eixler, S., Selig, U., and Karsten, U.: Extraction and detection methods for polyphosphate storage in autotrophic planktonic organisms, Hydrobiologia, 533, 135-143, 10.1007/s10750-004-2406-9, 2005.

Elbert, W., Weber, B., Burrows, S., Steinkamp, J., Budel, B., Andreae, M. O., and Poschl, U.: Contribution of cryptogamic covers to the global cycles of carbon and nitrogen, Nature Geosci, 5, 459-462, http://www.nature.com/ngeo/journal/v5/n7/abs/ngeo1486.html#supplementary-information, 2012.

Ernst, A., and Boger, P.: Glycogen accumulation and the induction of nitrogenase activity in the heterocyst-forming cyanobacterium Anabaena-variabilis, Journal of General Microbiology, 131, 3147-3153, 1985.
Garcia-Pichel, F., and Belnap, J.: Microenvironments and microscale productivity of cyanobacterial desert crusts, J Phycol, 32, 774-782, 1996.
Garcia-Pichel, F., Belnap, J., Neuer, S., and Schanz, F.: Estimates of global cyanobacterial biomass and its distribution, Arch Hydrobiol Suppl Alg Studies, 213-228, 2002.
Garcia-Pichel, F., and Wojciechowski, M. F.: The Evolution of a Capacity to Build Supra-Cellular Ropes Enabled Filamentous Cyanobacteria to Colonize Highly Erodible Substrates, Plos One, 4, 10.1371/journal.pone.0007801, 2009.
Garcia-Pichel, F., Loza, V., Marusenko, Y., Mateo, P., and Potrafka, R. M.: Temperature Drives the Continental-Scale Distribution of Key Microbes in Topsoil Communities, Science, 340, 1574-1577, 10.1126/science.1236404, 2013.
Grote, E. E., Belnap, J., Housman, D. C., and Sparks, J. P.: Carbon exchange in biological soil crust communities under differential temperatures and soil water contents: implications for global change, Global Change Biology, 16, 2763-2774, 10.1111/j.1365-2486.2010.02201.x, 2010.
Henry, C. S., DeJongh, M., Best, A. A., Frybarger, P. M., Linsay, B., and Stevens, R. L.: High-throughput generation, optimization and analysis of genome-scale metabolic models, Nature Biotechnology, 28, 977-U922, 10.1038/nbt.1672, 2010.
Hokputsa, S., Hu, C. X., Paulsen, B. S., and Harding, S. E.: A physico-chemical comparative study on extracellular carbohydrate polymers from five desert algae, Carbohydrate Polymers, 54, 27-32, 10.1016/s0144-8617(03)00136-x, 2003.
Johnson, S. L., Kuske, C. R., Carney, T. D., Housman, D. C., Gallegos-Graves, L. V., and Belnap, J.: Increased temperature and altered summer precipitation have differential effects on biological soil crusts in a dryland ecosystem, Global Change Biology, 18, 2583-2593, 10.1111/j.1365-2486.2012.02709.x, 2012.
Kanehisa, M., and Goto, S.: KEGG: kyoto encyclopedia of genes and genomes, Nucleic Acids Res, 28, 27-30, 2000.
Karp, P. D., Riley, M., Paley, S. M., and Pellegrini-Toole, A.: The MetaCyc Database, Nucleic Acids Research, 30, 59-61, 2002.
Maestre, F. T., Delgado-Baquerizo, M., Jeffries, T. C., Eldridge, D. J., Ochoa, V., Gozalo, B., Quero, J. L., Garcia-Gomez, M., Gallardo, A., Ulrich, W., Bowker, M. A., Arredondo, T., Barraza-Zepeda, C., Bran, D., Florentino, A., Gaitan, J., Gutierrez, J. R., Huber-Sannwald, E., Jankju, M., Mau, R. L., Miriti, M., Naseri, K., Ospina, A., Stavi, I., Wang, D., Woods, N. N., Yuan, X., Zaady, E., and Singh, B. K.: Increasing aridity reduces soil microbial diversity and abundance in global drylands, Proc Natl Acad Sci U S A, 112, 15684-15689, 10.1073/pnas.1516684112, 2015a.
Maestre, F. T., Escolar, C., Bardgett, R. D., Dungait, J. A., Gozalo, B., and Ochoa, V.: Warming reduces the cover and diversity of biocrust-forming mosses and lichens, and increases the physiological stress of soil microbial communities in a semi-arid Pinus halepensis plantation, Front Microbiol, 6, 865, 10.3389/fmicb.2015.00865, 2015b.
Orth, J. D., Thiele, I., and Palsson, B. O.: What is flux balance analysis?, Nature Biotechnology, 28, 245-248, 10.1038/nbt.1614, 2010.
Overbeek, R., Olson, R., Pusch, G. D., Olsen, G. J., Davis, J. J., Disz, T., Edwards, R. A., Gerdes, S., Parrello, B., Shukla, M., Vonstein, V., Wattam, A. R., Xia, F., and Stevens, R.: The SEED and the Rapid Annotation of microbial genomes using Subsystems Technology (RAST), Nucleic Acids Research, 42, D206-D214, 10.1093/nar/gkt1226, 2014.
Potts, M.: Mechanisms of desiccation tolerance in cyanobacteria, European Journal of Phycology, 34, 319-328, 10.1017/s0967026299002267, 1999.
Rajeev, L., da Rocha, U. N., Klitgord, N., Luning, E. G., Fortney, J., Axen, S. D., Shih, P. M., Bouskill, N. J., Bowen, B. P., Kerfeld, C. A., Garcia-Pichel, F., Brodie, E. L., Northen, T. R., and Mukhopadhyay, A.: Dynamic cyanobacterial response to hydration and dehydration in a desert biological soil crust, Isme Journal, 7, 2178-2191, 10.1038/ismej.2013.83, 2013.
Reed, S. C., Coe, K. K., Sparks, J. P., Housman, D. C., Zelikova, T. J., and Belnap, J.: Changes to dryland rainfall result in rapid moss mortality and altered soil fertility, Nature Climate Change, 2, 752-755, 10.1038/nclimate1596, 2012.
Swenson, T. L., Jenkins, S., Bowen, B. P., and Northen, T. R.: Untargeted soil metabolomics methods for analysis of extractable organic matter, Soil Biology and Biochemistry, 80, 189-198, https://doi.org/10.1016/j.soilbio.2014.10.007, 2015.
Vu, T. T., Stolyar, S. M., Pinchuk, G. E., Hill, E. A., Kucek, L. A., Brown, R. N., Lipton, M. S., Osterman, A., Fredrickson, J. K., Konopka, A. E., Beliaev, A. S., and Reed, J. L.: Genome-Scale Modeling of Light-Driven Reductant Partitioning and Carbon Fluxes in Diazotrophic Unicellular Cyanobacterium Cyanothece sp ATCC 51142, Plos Computational Biology, 8, 10.1371/journal.pcbi.1002460, 2012.

Knoop, H., Gründel, M., Zilliges, Y., Lehmann, R., Hoffmann, S., Lockau, W., and Steuer, R.: Flux Balance Analysis of Cyanobacterial Metabolism: The Metabolic Network of Synechocystis sp. PCC 6803, PLOS Computational Biology, 9, e1003081, 10.1371/journal.pcbi.1003081, 2013.

Yin, Z., Wilson, S., Hauser, N. C., Tournu, H., Hoheisel, J. D., and Brown, A. J.: Glucose triggers different global responses in yeast, depending on the strength of the signal, and transiently stabilizes ribosomal protein mRNAs, Mol Microbiol, 48, 713-724, 2003.

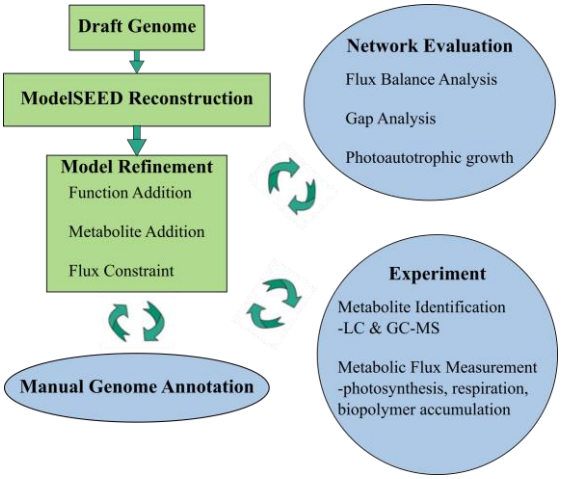

Figure 1: Metabolic reconstruction process diagram.

450

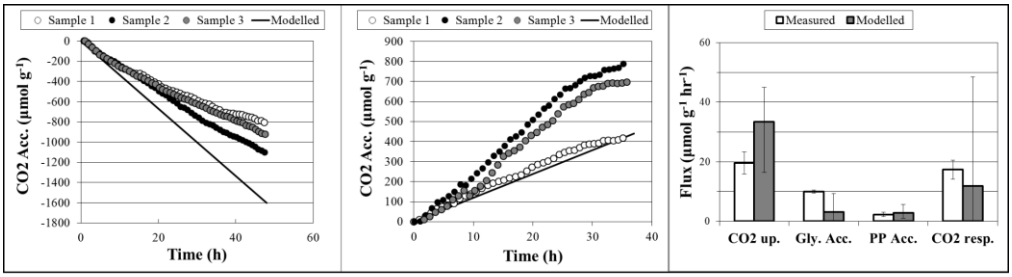

(a) (b) (c)

Figure 2: Comparisons of experimental and modelled CO_2 accumulation (a) in the light, where a negative value indicates uptake, and (b) in the dark, where a positive value indicates respiration. Biopolymer and CO_2 flux rates are compared in (c), where error bars on modelled flux rates are the upper and lower bounds determined through sensitivity analysis; error bars on measured flux rates are standard deviations.

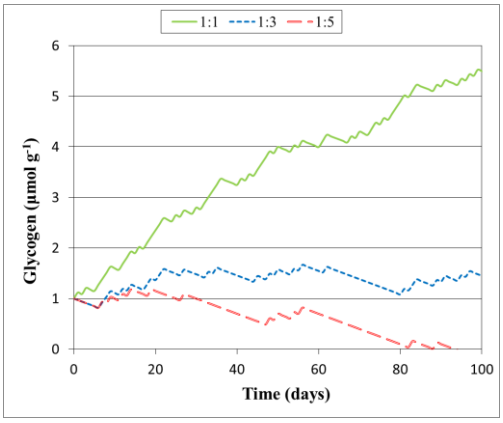

Figure 3: Predicted glycogen depletion over 1 month under three climate scenarios, where the ratio of light:dark wetting events are 1:1, 1:3, and 1:5.

Table 1: Comparison of curation and automated annotation.

Major manually curated pathways	Predicted in curation	Predicted in RAST annotation
All amino acid biosynthetic pathways	x	x
Ammonium Assimilation	x	x
Bifidobacterium Shunt	x	x
Heterolactic Acid Fermentation		
Homolactic Acid Fermentation	x	x
Mixed Acid Fermentation		
Nucleoside triphosphate biosynthetic pathways	x	x
Photosynthetic light reactions	x	
Calvin Cycle	x	x
Nitrate Assimilation	x	
Nitrogen Fixation		
Glycogen Biosynthesis	x	
Glycolysis	x	x
Hydrogen Production		
Pentose Phosphate Cycle	x	x
Sulfur and Sulfate Reduction	x	x
TCA Cycle	x	x
Peptidoglycan Biosynthesis	x	x
β-polyhydroxybutyrate synthesis	x	
Cyanophycin synthesis	x	
Polyphosphate synthesis	x	

Table 2: Modelled Biopolymer Reactions.

Reaction	Description
ATP ←→ADP + Polyphosphate	Polyphosphate synthesis/degradation
Polyphosphate ←→ Nothing	Polyphosphate sink
Glucose-1-phosphate ← Phosphate + H(+) + Glycogen	Glycogen degradation
ADP-Glucose → Glycogen + ADP	Glycogen synthesis
Glycogen ←→Nothing	Glycogen Sink
(R)-3-Hydroxybutanoyl-CoA ←→ CoA+PHB	PHB synthesis/degradation
PHB←→Nothing	PHB sink

Table 3: Experimental and modelled flux values over light and dark conditions. Constraint fluxes are noted with a "*". Negative and positive CO_2 fluxes represent uptake and respiration respectively, while negative and positive biopolymer flux rates represent depletion and accumulation respectively. Measured "-" and "+" refer to the standard deviation. Modelled "-" and "+" refer to the upper and lower values obtained from sensitivity analysis. In modelled constraint reactions for light, "-" and "+" represent the assumed deviation that is input into sensitivity analysis.

	Measured			Modeled		
	Flux (µmol g^{-1} h^{-1})	~~LB~~ -	~~UB~~ +	Flux (µmol g^{-1} h^{-1})	~~LB~~ -	~~UB~~ +
Light (1)						
Light*	141			141	93	211
CO_2	-19.6	-23.3	-15.9	-33.4	-50.3	-21.8
Light (2)						
Light*	4670			4670	3551	6290
Glycogen	9.99	9.47	10.51	3.07	0.00	9.30
PHB	0.0366	0.0050	0.0683	0.121	0.044	0.250
Polyphosphate	2.28	1.57	2.99	2.82	1.00	5.70
Dark						
Light*	0.00			0.00		
Glycogen*	-2.49	-6.08	1.09	-2.49	-9.66	4.67
PHB*	-0.14	-0.17	-0.11	-0.136	-0.20	-0.07
Polyphosphate*	-0.02	-1.27	1.22	-0.02	-2.51	2.46
CO_2	17.3	14.1	20.6	11.9	0	48.5